High Rate Deposition of 5 μm Thick $YBa_2Cu_3O_7$ Films Using the BaF_2 Ex-situ Post Annealing Process

Vyacheslav F. Solovyov, Harold J. Wiesmann, Li-jun Wu and Masaki Suenaga
Department of Applied Science, Brookhaven National Laboratory, Upton, NY 11973

Ron Feenstra
Solid State Division, Oak Ridge National Laboratory, Oak Ridge, TN 37831

***Abstract*—We have investgated the crystallization of thick YBCO films under various annealing conditions. The films were deposited by high-rate co-evaporation of Y, Cu and BaF_2 onto room-temperature $SrTiO_3$ substrates at rates exceeding 10 nm/s. TEM microscopy was performed to establish the microscopic structure of partially processed films and help elucidate the growth mechanism. *In-situ* resistivity measurements were used to monitor the crystallization of the YBCO films during the annealing process. Resistivity measurements and TEM microscopy of samples at different stages of the film growth are compared. Our results indicate that, in addition to oxygen partial pressure, water vapor pressure is an important parameter which defines the dynamics of film growth and crystallization. 5 μm thick films with $J_c > 2 \times 10^5$ A/cm^2 (1 T $H\|c$) have been fabricated.**

I. Introduction

$YBa_2Cu_3O_7$ (YBCO) has demonstrated promising superconducting properties for use at liquid nitrogen temperatures with $J_c(77\ K) > 10^6$ A/cm^2 and $H_{irr}(77\ K) \approx 7$ T. Recent progress in the development of bi-axially oriented epitaxial buffer layers on flexible metal substrates [1], [2] has opened up possibilities for the application of YBCO in electric utility and high magnetic field devices.

Post-annealing using the barium fluoride process is a viable alternative to laser ablation and MOCVD for manufacturing textured YBCO coated conductors. The advantage of the barium fluoride post-annealing technique [3] is that it divides the YBCO deposition and film crystallization into separate steps, allowing for high deposition rates > 10 nm/s. Stable *c*-axis growth is achieved by annealing in oxygen partial pressures much lower than for *in-situ* techniques [4] and the BaF_2 is decomposed by humidifying the annealing atmosphere. Under these annealing conditions we have previously grown 3 μm thick films with $J_c = 2 \times 10^5$ A/cm^2 ($H\|c = 1$ T) [5]. There is still no clear understanding of the factors influencing the growth speed and no systematic estimation of the growth rate under various conditions was made. Also it is not known whether 5 – 10 μm thick *c*-axis oriented films can be produced by this method or whether critical currents high enough for coated conductor applications can be achieved.

In this paper we analyze the effect of variations of the post-annealing process as regards the growth kinetics and critical currents. In the first section we report on the results of *in-situ* resistivity measurements as a method for monitoring the growth kinetics of the films during the post-annealing process. Data on the film growth rate as a function of temperature and water vapor pressure are also presented. In the second section we present results of critical current transport measurements of 1 and 5 μm thick YBCO films.

II. Experimental

Precursor films of the approximate stoichiometric cation composition Y:Ba:Cu = 1:2:3 were deposited on 3 mm ×10 mm (100) $SrTiO_3$ substrates without external heating in a vacuum chamber. The Y and Cu were deposited using Temescal 14 kW electron beam guns and a custom 300 W thermal evaporation source was used to deposit the BaF_2. The deposition rate was 14 nm/s as calculated for the thickness of annealed YBCO films. The background pressure in the chamber was $1 - 2 \times 10^{-6}$ Torr during deposition and the deposition rates of the individual sources were controlled by Inficon quartz crystal rate monitors. The reproducibility of the composition of the films was 5 - 10% from run to run. The composition was confirmed by measuring Y:Ba:Cu molar ratios of selected films using Rutherford Back Scattering and inductively coupled plasma spectroscopy.

Post deposition annealing was performed in a quartz tube. The annealing atmosphere was synthesized by mixing certified gases using electronic mass flow controllers. The total gas flow was fixed at 100 cm^3/min and was humidified by bubbling through a heated water bath. The humidity was measured with a thin film polymer capacitive sensor and active feedback was used to stabilize the water vapor partial pressure by varying the water bath temperature.

Routine characterization included $\theta - 2\theta$ powder X-ray diffractometry and critical current transport measurements in magnetic field of up to 7 T with the option of sample rotation with respect to the magnetic field. The critical current was inferred from *I-V* curves using a 1 μV/cm electric field strength criterion.

III. Kinetics of the Film Growth

It is assumed [3] that the basic reaction underlying the

Manuscript received on September 15, 1998.
The work at Brookhaven National Laboratory was performed under the auspices of U. S. Department of Energy, contract No. DE-AC02-98CH10886 and that at Oak Ridge National Laboratory was sponsored by the Division of Materials Science, U. S. Department of Energy under contract No. DE-AC-05-96OR22464.

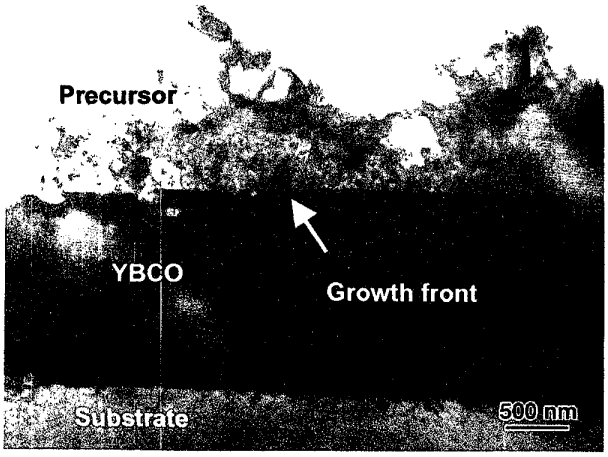

Fig. 1. TEM micrograph of half-processed 3 μm film. Annealing temperature 725 °C, water vapor pressure 25 Torr, oxygen presure 100 mTorr.

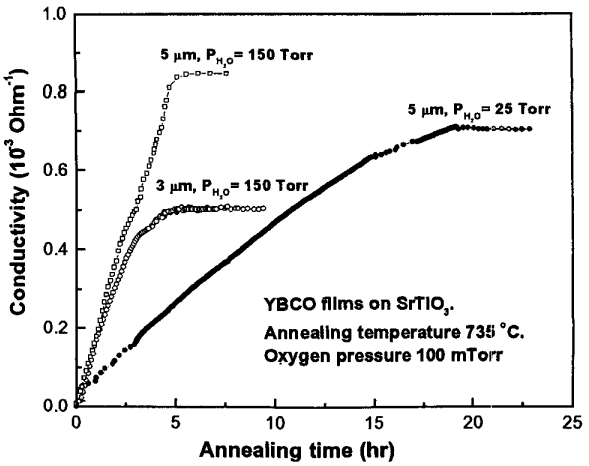

Fig. 2. Conductivity versus annealing time of thick-film samples during annealing at 735 °C, 100 mT oxygen pressure and various water vapor pressure values. The lines connecting points are guides for an eye.

post-annealing process is the reduction of BaF_2 to BaO with the release of HF and the oxidation of Y and Cu to Y_2O_3 and CuO with subsequent formation of YBCO. Epitaxial growth becomes possible because YBCO has lower thermodynamic potential on the substrate than in the bulk. Growth proceeds as a uniform advancement of the YBCO-precursor film interface from the substrate towards the surface of the film. Fig. 1 is a TEM micrograph of a 3 μm film, which was quenched at the point where the crystallization front reached approximately 1/2 of the thickness of the film. A sharp interface can be seen, dividing the epitaxial YBCO and the precursor films. The precursor film was determined by selected area diffraction to be a mixture of nanocrystals of CuO, Y_2O_3 and BaF_2. Detailed study of the interface revealed an amorphous layer approximately 10 nm thick. The amorphous layer indicates that a liquid phase exists at the interface and acts as a flux [6].

Since the precursor film is an insulator and YBCO is a conductor, measurements of the film resistivity during annealing provide information regarding the growth dynamics. The film resistivity drops as more precursor material is converted into YBCO. The intrinsic resistivity of YBCO itself differs, especially in the presence of *a*-axis oriented grains, which occur in mixed *c*-axis, *a*-axis oriented growth. Thus, aside from a general monitoring of the growth process, *in-situ* resistivity measurements allow us to determine whether *a*-axis oriented grains are present in growing YBCO film. Annealing curves plotted as sample conductivity versus annealing time are shown in Fig. 2. The interpretation of the data is as follows: the linear region corresponds to the increase in the YBCO thickness as the growth front travels from the substrate to the film surface. The plateau indicates completion of the growth process. The linear parts of the 3 and 5 μm annealing curves are coincident demonstrating that the growth kinetics is controlled by the reaction interface. It is also observed that water vapor pressure is an essential factor controlling the growth rate of the films. An increase of the water vapor pressure from 25 to 150 Torr (see corresponding curves in Fig. 2) increases the growth rate by a factor of 3. Table I summarizes data on in-situ resistivity measurements of 3 – 5 μm thick films. The growth rate is presented as a function of the annealing temperature, T_A, and the water vapor pressure, P_{H2O}. The oxygen partial pressure, P_{O2}, was optimized for maximum suppression of *a*-axis growth at the given temperature and is included in the table for reference:

TABLE I

GROWTH RATE DEPENDENCE ON ANNEALING TEMPERATURE AND WATER VAPOR PRESSURE

T_A (°C)	P_{o2} (mTorr)	P_{H2O} (Torr)	Growth rate (Å/s)
725	100	25	0.7
725	100	150	1.8
735	100	25	0.7
735	100	150	2.5
800	300	25	2.3
800	300	150	6.0

It can be concluded from the data that temperature and water vapor pressure are the main factors influencing the growth rate. As far as film performance is concerned, higher growth rates result in less *a*-axis oriented regions and randomly oriented grains. Indeed, it may be noted from Fig. 2 that the film annealed at 25 Torr has lower conductivity than the one annealed at 150 Torr. X-ray diffractometry confirmed a considerable content of *a*-axis oriented grains in the 25 Torr sample, while the film annealed at 150 Torr was almost completely *c*-axis oriented. Thus, a high growth rate, induced by a high water vapor pressure, can produce thick *c*-axis oriented films even at temperatures as low as 720 °C. The suppression of *a*-axis oriented growth can also be achieved by annealing at elevated temperature, e.g. 800 °C, but as we will

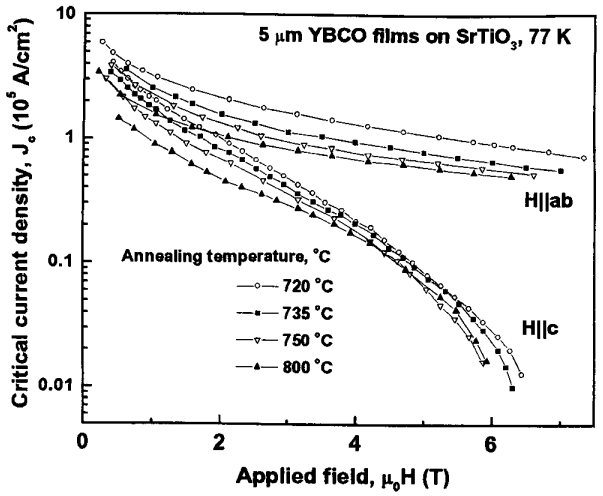

Fig. 3. Critical current density field dependences of 5 μm thick YBCO samples on $SrTiO_3$ for $H||c$ and $H||ab$ orientations at the liquid nitrogen temperature. The samples were annealed at 720, 735, 750 and 800 °C. The lines are guides for an eve.

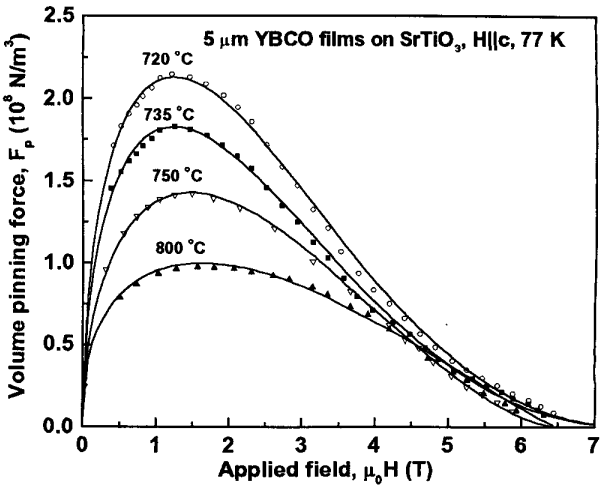

Fig. 4. Field dependence of the volume pinning force F_p of 5 μm samples annealed at at 720, 735, 750 and 800 °C. The lines are approximations by Kramer's scaling law.

show in the next section, a reduced density of pinning centers causes lower J_c's.

We have found a minor influence of the oxygen partial pressure on the growth rate, even though at high oxygen pressures the growth mode changes from *c* to *a*-axis oriented.

IV. Critical Currents of Post-Annealed Films

Fig. 3 shows the field dependence of the critical current density of 5 μm thick samples annealed at 720, 735, 750 and 800 °C. For samples annealed at 720, 735 and 750 °C, P_{O2} = 100 mTorr and P_{H2O} = 150 Torr. For the 800 °C sample the oxygen pressure was set at the optimum value, 300 mTorr, and the water vapor pressure was maintained at 50 Torr to achieve a growth rate of approximately 2.5 Å/s, the same growth rate as for the other samples. According to XRD all the samples were *c*-axis oriented and therefore observed variations of J_c cannot be attributed to *a*-axis oriented grains. We observed considerable increase of the critical current as T_A decreases for both $H||c$ and $H||ab$ orientations. It may be observed from Fig. 3 that the enhancement of J_c is most prominent for fields below 3 T with $H||c$.

The volume pinning force, $F_p=J_c \times H$, versus applied magnetic field ($H||c$) is plotted in Fig. 4 for 5 μm thick films annealed at four different temperatures. In order to better understand the influence of the annealing temperature on J_c the pinning force data were approximated using Kramer's scaling law $F_p \propto b^p \times (1-b)^q$ [7]. Here $b = H / H_{irr}$, and p, q and H_{irr} are fitting parameters. The best fit to the data is shown in Fig. 4 as solid lines. The fitting parameters along with J_c values are listed in Table II. H_{irr} is identified as the irreversibility field, since at this field the pinning strength is approximately zero. The data suggest that lower annealing temperatures result not only in higher J_c's but also in higher irreversibility fields.

TABLE II

Critical Currents Densities and Approximation Parametrs of 5 μm Thick Films Annealed at Various Temperatures

T_A (°C)	J_c (10^5 A/cm^2) at $\mu_0 H\|\|c$ = 1 T	J_c (10^5 A/cm^2) at $\mu_0 H\|\|ab$ = 1 T	p	q	$\mu_0 Hirr$ (T) H||c
720	2.0	3.3	0.5	2.6	7.7
735	1.7	2.6	0.5	2.2	7.4
750	1.0	2.3	0.5	1.7	6.5
800	0.9	1.5	0.4	1.2	6.4

The average values of the indexes are close to p = 0.5 and q = 2 which is predicted by the flux-shear model [7]. The functional dependence, $F_p \propto b^{0.5} \times (1-b)^2$, has been observed for wide variety of low-temperature superconductors such as Nb_3Sn [8] and in high-temperature superconductors [9]. In the framework of the flux-shear model the pinning is determined by planar boundaries and the critical state is reached when the flux lattice starts to percolate in between the boundaries. Although we lack the systematic TEM data needed to identify the details of the relevant boundaries in our samples, surface SEM photomicrographs, as shown in Fig. 5, might give some insight into the possible correlation between annealing conditions and film microstructure. TEM microphotographs reveal that the surface features of Fig. 5 are raised terraces on the order of 50 nm in height. For the 800 °C film the terraces have a micron-scale length but the size of the terraces shrinks down to submicron size for the 725 °C sample. If the films grow via nucleation and coalescence of these terraces then it is possible to attribute the pinning enhancement at low T_A to a higher density of low angle intergrain boundaries. However we do not yet have any TEM evidence that the surface morphology is representative of film growth via coalescing terraces or what type of defect is formed. Other possible

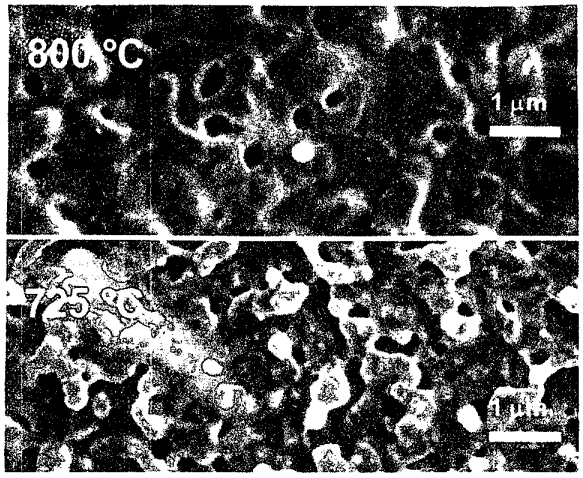

Fig. 5. SEM micrograph of surface of 1mm films processed at 725 and 800 °C. Note different surface morphology.

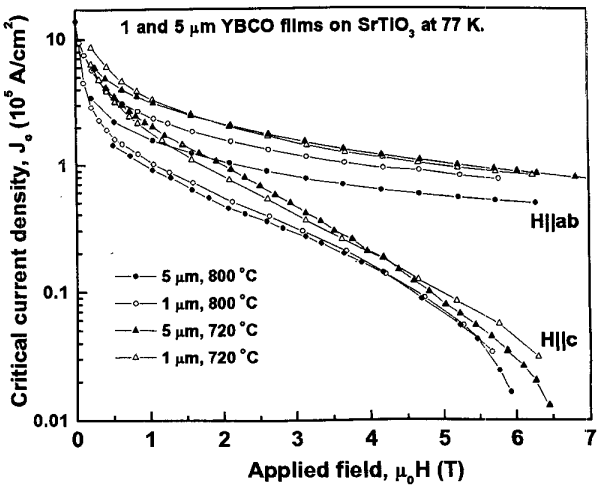

Fig. 6. Comparison of the critical current densities of 5 and 1 μm thick films grown at 720 and 800 °C for $H||c$ and $H||ab$ orientations.

planar pinning sites are twin boundaries [10] which were observed to have 40 nm spacing for a film grown at 750 °C. However, at this time we do not have systematic observations of the variation in twin boundary spacing with annealing temperature. It should be noted that regardless of the pinning mechanism, a reduction in T_A enhances the pinning for thick films in both field orientations, $H||c$ and $H||ab$.

The dependence of $J_c(H)$ on applied magnetic field for films 1 and 5 μm thick with $H||c$ and $H||ab$ are shown in Fig. 6. There is almost no change in J_c for 1 and 5 μm thick films grown at 800 and 720 °C when measured with $H||c$. For $H||ab$ 5 μm thick films grown at 800 °C have lower critical currents than 1 μm thick films grown at the same temperature. We have observed this behavior for films 1 – 5 μm thick grown at 750 and 735 °C. Only by reducing the annealing temperature below 725 °C does J_c become independent of the thickness for $H||ab$ as shown in Fig. 6.The independence of J_c with film thickness for $H||c$ suggests that the pinning centers are uniformly distributed from the YBCO- substrate interface to the film surface. This is consistent with the data of Fig. 3 and the application of Kramer's scaling law, and the inference that the pinning centers might be planar boundaries. For the field orientation $H||ab$ the data is consistent with a maximum density of pinning centers at the substrate. A decrease in the density of pinning centers away from the substrate has previously been reported [6]. These centers might be stacking faults, which can be described as planar boundaries parallel to the *ab* plane. Regardless of the type of defect responsible for pinning it is important to note, that for films grown at 720 °C, J_c becomes independent of the film thickness which suggests that another unidentified defect controls the pinning.

V. Conclusion

In conclusion we have shown that 5 um thick YBCO films having high critical currents, > 10^6 A/cm^2 in zero field and > 10^5 A/cm^2 at 1 Tesla, can be made by the BaF_2 post annealing process. Resistivity measurements made *in-situ* can be effectively used for monitoring the epitaxial growth of YBCO during post-annealing. For the first time we have used in-situ resistivity data to measure the growth rate of YBCO under various annealing conditions. Low temperature annealing was shown to result in films with high J_c, where J_c was independent of the film thickness for the technologically important $H||c$ orientation.

References

[1] X.D. Wu *et al*, "Properties of $YBa_2Cu_3O_{7-\delta}$ thick films on flexible buffered metallic substrates", *Appl. Phys. Lett.*, vol. 67, pp. 2397-2399, October 1995.

[2] M. Paranthaman *et al*, "Growth of biaxially textured buffer layers on rolled-Ni substrates by electron-beam evaporation", *Physica C*, vol 275, pp. 266-272, March 1997.

[3] P.M. Mankiewich *et al*, "Reproducible technique for fabrication of thin films of HTSC", *Appl. Phys. Lett.*, vol. 51, pp. 1753-1755, November 1987.

[4] R. Feenstra, T. Lindermer, J.D. Budai, and M. D. Golloway, "Effect of oxygen pressure on the synthesis of $YBa_2Cu_3O_{7-x}$ thin films by post-deposition process", *J. Appl. Phys.*, vol. 69 pp. 6569-6572, April 1991.

[5] V. F. Solovyov, H. J. Wiesmann, M. Suenaga, and R. Feenstra,"Thick $YBa_2Cu_3O_7$ films by post annealing of the precursor by high rate e-beam deposition on $SrTiO_3$ substrates", *Physica C*, in press.

[6] P.C. McIntre, M.J. Cima and A. Roshko, "Epitaxial nucleation and grows of chemically derived $Ba_2YCu_3O_{7-x}$ thin films on (001) $SrTiO_3$", *J. Appl. Phys.*, vol. 77, pp.5263-5271, May 1995.

[7] E.J. Kramer, "Scaling laws for flux pinning in hard superconductors", *J. Appl. Phys.*, vol. 44, pp.1360-1370, March 1973.

[8] M. Suenaga, *Superconductor material science*, S. Foner and B.B. Swartz, Eds., New York: Plenum press, 1981, p. 201.

[9] T. Nishikazu *et al*, "Transport critical currents and flux pinning mechanisms in single-crystalline thin films $YBa_2Cu_3O_{7-\delta}$", *Physica C*, vol. 181, pp. 223-232, November 1991.

[10] H. Safar *et al*, "*ab*-plane anisotropy of the critical currents in twinned $YBa_2Cu_3O_{7-\delta}$", *Appl. Phys. Lett.*, vol. 68, pp.1853-1855, March 1996.